Dynamic Mechanical Analysis of the Effect of Water on Glass Bead–Epoxy Composites

JO-YU WANG[1] and HARRY J. PLOEHN[2,*]

[1]Offshore Technology Research Center, Texas A&M University, College Station, Texas 77843, and [2]Department of Chemical Engineering, University of South Carolina, Swearingen Engineering Center, Columbia, South Carolina 29208

SYNOPSIS

Dynamic mechanical analysis (DMA) has been used to investigate the effect of water and glass bead surface treatment on the properties of glass bead–epoxy composites. By treating or not treating the glass beads with a silane coupling agent, we fabricated composites with ostensibly good or poor interfacial adhesion. SEM images of fracture surfaces and water uptake data confirmed this picture. We used dynamic mechanical tests to measure the material properties of dry and wet specimens. Temperature sweep tests of atmosphere-conditioned specimens indicated that the value of the loss tangent at the temperature of the α-relaxation peak was most sensitive to interfacial adhesion. For wet specimens, the magnitude of an additional relaxation process, denoted as the ω-relaxation, correlated strongly with water uptake and, indirectly, interfacial adhesion. Master curves constructed from frequency sweep tests also manifested differences among dry and wet specimens, but shift factor data suggested that these tests were more prone to complications due to water loss. Apparent activation energies of α- and β-relaxation processes were statistically significant indicators of interfacial adhesion in dry and wet composites, respectively. © 1996 John Wiley & Sons, Inc.

INTRODUCTION

The effect of water on the mechanical properties and durability of polymer–matrix composites will decide their feasibility for use in composite risers and other structures for deep water offshore oil recovery. Water alters the properties of the polymeric matrix[1] and degrades reinforcing fibers, especially glass.[2,3] A growing body of evidence indicates that water has a distinct influence upon the matrix–fiber interphase.[3,4]

Distinguishing the effects of water on interphases from those on the bulk phases is a key characterization issue. Static mechanical and dynamic fatigue tests[5] tell us much about damage mechanisms and properties such as strength, stiffness, and creep, but these methods do not isolate the influence of surface treatment or water on the fiber–matrix interface.[16] Single fiber micromechanical tests attempt to measure interfacial strength directly, but various types of tests give inconsistent results.[6] Of these, the single-fiber pull-out test clearly reveals the effect of water on fiber–matrix debonding[7] but only provides an apparent interfacial shear strength. Schutte[22] has recently reviewed the use of single-fiber tests to examine water-induced changes in interfacial adhesion.

Dynamic mechanical analysis (DMA) has been used to study interfacial effects in both particulate- and fiber-reinforced polymer–matrix composites.[8–24] Most of this work[9–18] characterizes the relationship between surface treatment of the reinforcement and dynamic mechanical properties. A few studies[18–20,23] have used DMA to characterize the effect of water on the interphase. We are not aware of any previous work that relates variations in both reinforcement surface treatment and water content to dynamic mechanical properties.

The objective of this work was to synthesize glass bead–epoxy composites with ostensibly poor and good interfacial adhesion. We used glass bead reinforcement rather than fibers to avoid complica-

* To whom correspondence should be addressed.

Journal of Applied Polymer Science, Vol. 59, 345–357 (1996)
 CCC 0021-8995/96/020345-13

tions of fiber orientation and anisotropic water diffusion. We conditioned neat cured resin, composites with clean glass beads, and composites with silane-treated glass beads in deionized water. We then performed a comprehensive set of dynamic mechanical tests on all classes of specimens, both dry and wet. Our ability to rationalize variations in the dynamic mechanical properties in terms of glass bead surface treatment and water content illustrate the utility of DMA for characterizing the effect of water on interfacial adhesion.

DYNAMIC MECHANICAL ANALYSIS

General Principles

Most textbooks explain the basic principles of dynamic mechanical analysis (DMA).[21] In the tensile mode, we subject a specimen to sinusoidal tensile elongation and measure the force required to achieve the deformation. Knowing the dimensions of the specimen enables us to convert the elongation and force into tensile strain (amplitude γ^0) and stress (σ) related by

$$\sigma = \gamma^0(E' \sin \omega t + E'' \cos \omega t), \quad (1)$$

which defines the frequency-dependent tensile storage and loss moduli E' and E''. The measured stress lags behind the applied strain by an amount $\delta(\omega)$ so that

$$\sigma = \sigma^0 \sin(\omega t + \delta) \quad (2)$$

in terms of the stress amplitude σ^0. Expanding the double angle in eq. (2) and comparison with eq. (1) indicates that

$$E' = \frac{\sigma^0}{\gamma^0} \cos \delta \qquad E'' = \frac{\sigma^0}{\gamma^0} \sin \delta \quad (3)$$

and defines

$$\tan \delta = \frac{E''}{E'} \quad (4)$$

as the loss tangent.

DMA characterizes the changes in E', E'', and tan δ due to variations in strain amplitude γ^0, oscillation frequency ω, and temperature T. Small values of γ^0, as determined by a strain sweep experiment at constant ω and T, ensure linear viscoelastic behavior for which E' and E'' are independent of γ^0. Temperature sweep experiments at constant γ^0 and ω identify polymer relaxation processes associated with energy dissipation. Data from frequency sweep experiments at constant γ^0 and a series of temperatures can be transformed into master curves via time–temperature superposition.[21] Master curves express dynamic mechanical data in an economical form and enable predictions of properties at temperatures and time scales beyond our experimental capabilities.

DMA Studies of Composite Interphases

Several groups have employed DMA to characterize the effect of fiber surface treatments on dynamic mechanical properties.[9–14,16,18] Most of these studies utilized only temperature sweep experiments. The feature that was most sensitive to the interphase was the height of the main loss tangent peak ($\tan\delta_\alpha$) found at a temperature (T_α) near the glass transition. Experiments involving glass beads[9,11,12] and glass fibers[10] showed that reactive aminosilane surface treatments decreased $\tan\delta_\alpha$. Reactive treatments presumably create better interfacial adhesion than can be achieved using unreactive treatments or none at all. Chua's work[10] provides the clearest support for this hypothesis: he observed an inverse correlation between $\tan\delta_\alpha$ and the apparent interfacial shear strength measured by the short-beam shear test (ASTM D2344).

Results from experiments on carbon fiber composites[13–17] cannot be interpreted as clearly because a variety of surface treatments, some of them proprietary, have been used. For composites containing carbon fibers that were dip-coated with reactive elastomers,[13] the interphase produced an extra peak in the relaxation spectra, but different amounts of elastomeric coating did not significantly change T_α or $\tan\delta_\alpha$. Harris et al.[14] used temperature sweep experiments to study a wide variety of carbon fiber surface treatments. They saw significant variations of $\tan\delta_\alpha$ for different classes of treatments, but the results could not be rationalized in terms of interfacial microstructure. Kennedy et al.[16] used frequency sweep tests to differentiate between composites containing untreated and treated carbon fibers. However, careful statistical analysis showed that presumably small differences in interfacial adhesion could not be distinguished by storage modulus, loss modulus, or loss tangent. The proprietary nature of the carbon fiber surface treatments precluded further analysis.

In general, DMA studies of composites with different surface treatments indicate greater values of T_α for composites compared to neat resin and for surface-treated compared to untreated reinforcement. However, the small magnitudes of the variations, their statistical uncertainty, and the incon-

sistency of the trends make it difficult to draw any conclusions from observations of T_α. Likewise, variations in storage modulus (tensile or shear) cannot discriminate among composites with different surface treatments. In contrast, several studies have shown that $\tan\delta_\alpha$ varies considerably with surface treatment in both glass- and carbon-reinforced composites. In glass-based composites, decreases in $\tan\delta_\alpha$ can reasonably be attributed to chemical bonding of sizing agents to both matrix and reinforcement. However, a mechanistic interpretation for carbon fiber composites has not been clearly established.

Many groups have examined the uptake of water by glass–epoxy composites,[22] with appropriate attention given to measuring the mechanical properties of wet composites. Relatively few studies have used DMA to characterize the particular effect of water on interphases. Williams[19] exposed composites containing glass, carbon, and aramid fibers, as well as glass beads, to boiling water for extended periods, but he only reported loss tangent values at temperatures below 0°C, far from the glass transition.

Other studies have shown that the loss tangent at a fixed temperature increases markedly with the amount of water uptake[23] and the conditioning temperature.[20,23] The results of Marzi et al.[23] indicated that the loss tangents of wet composites were always greater than those of corresponding dry composites at the same temperature. Furthermore, the ratio of wet to dry loss tangent depended on the strength of interfacial adhesion as inferred from glass transition[24] and water uptake measurements. The composites with ostensibly better fiber–matrix adhesion absorbed less water and displayed smaller ratios of wet to dry loss tangent.

EXPERIMENTAL

Materials

All samples contained equal stoichiometric amounts of liquid epoxy prepolymer DER 331 [diglycidyl ether of bisphenol A (DGEBA), Dow Chemical] and amine curing agent DEH 24 [triethylene tetramine (TETA), Dow Chemical]. Unit stoichiometry requires 12.9 parts per hundred parts of resin (phr) of TETA with respect to DGEBA. Dow Chemical recommends this resin and curing agent for common ambient cure applications.

The composite samples incorporated precision grade glass beads (Cataphote) containing 71–74% by weight of SiO_2. Scanning electron microscopy confirmed the 40 μm average bead diameter reported by the manufacturer. The coupling agent, GPS (3-glycidoxypropyltrimethoxysilane) (Aldrich) has epoxy and siloxane groups at either end of the molecule. The epoxy groups presumably reacted with amines in the curing agent. The siloxane groups hydrolyzed in aqueous solution to give siloxanol groups (Si—OH), which presumably formed ether bonds (Si—O—Si) with the silicon in the glass beads.

Specimen Preparation

We prepared three kinds of specimens: neat resin, composites containing cleaned glass beads, and composites containing glass beads treated with GPS. All composite specimens contained 40% glass beads by volume. The glass beads were cleaned by washing in isopropanol and vacuum drying for 1 h at 100°C. To coat the beads with silane coupling agent, we mixed clean beads with a 1% aqueous solution of GPS for 5 min. After removing excess solution by filtration, we heated the glass beads under vacuum for 1 h at 110°C. Sieving the beads before mixing with epoxy resin eliminated unwanted aggregates. We shall refer to composites prepared with clean beads and silane-coated beads as "untreated" and "treated," respectively.

We followed a carefully designed sequence of steps to minimize voids due to air bubbles, ensure good dispersion of glass beads, and obtain a uniform degree of cure. First, we dispersed the glass beads in epoxy resin heated to about 80°C. After cooling the mixture, we added the curing agent with thorough mixing. Twenty minutes of degassing in a vacuum oven at ambient temperature removed all air bubbles.

Our mold consisted of two vertical, Teflon-lined aluminum plates spaced with Teflon shims and rolled tape as a barrier to hold the mixture in the gap. After carefully pouring the mixture into the mold, we allowed 24 h for curing at ambient temperature. We then removed the plaque from the mold and cut it into specimens with dimensions ($0.8 \times 8 \times 40$ mm) suitable for subsequent testing. The samples were then postcured in the vacuum oven at elevated temperature.

The concept of the time–temperature–transformation (TTT) diagram[25] helped us establish a postcure schedule that gives the highest possible degree of cure without thermal degradation. Through a trial-and-error procedure[18] involving measurement of the glass transition temperature using DMA, we

fixed the postcure schedule as 26 h at a temperature of 124°C.

Specimen Conditioning

At least 10 cut and cured coupons of each class of specimen were stored and tested under ambient conditions. We call these "dry" specimens, although we know that they actually contained an unknown amount of water absorbed from the atmosphere.

At least 10 cut and cured coupons of each class of specimen were immersed in deionized water at ambient temperature for a minimum of 1000 h. To monitor water uptake, we removed the wet specimens from the water each day, wiped them thoroughly using a lint-free towel, and weighed them on an analytical balance. We refer to the water-saturated specimens as "wet."

Visual Characterization

We visualized fracture surfaces of dry composite specimens using scanning electron microscopy (JEOL T330A). The surfaces of some specimens were polished with fine sandpaper to expose beads just below the surface.

Dynamic Mechanical Measurements

The Rheometrics Solids Analyzer II (RSA II) characterizes the viscoelastic properties of solid materials in tension, compression, or bending. A servo motor applies an oscillatory strain to the test specimen, and a transducer measures the force required to effect the applied deformation. For tensile tests, the specimen is placed in the grips of the film/fiber fixture, taking care to properly align the specimen along the central axis of the motor and transducer shafts. A heat gun controls the temperature in the environmental chamber through forced convection of either vapor evaporating from liquid nitrogen or air passing over a heating element.

We performed strain, temperature, and frequency sweeps. We selected a strain (0.001) such that the specimens deformed within the linear viscoelastic range. The temperature sweep tests varied T between −105 to 170°C at a fixed frequency of 10 rad/s. A relatively large temperature ramp, 10°C/min, reduced the testing time without undue sacrifice of experimental accuracy. The frequency sweep tests varied T between 0.1 and 100 rad/s and at temperatures between −105 and 170°C, stepping upwards in increments of 7.5°C. Thermal soaking times of 3 and 6 min (for temperatures above and below ambient) minimized the effects of thermal transients and helped maintain water content during the course of the tests. In addition, we used a thin layer of high-vacuum silicone grease (Dow Corning) on wet specimens to reduce water loss accelerated by the forced convection of hot, dry gases.

We constructed master curves for all specimens by horizontally shifting the frequency sweep isotherms relative to a reference temperature of 145°C. This laborious procedure was facilitated by the use of RHIOS software (Rheometrics, Inc.). Time–temperature superposition (TTS) established the value of the shift factor a_T as a function of temperature with respect to the selected reference temperature.[21]

RESULTS

Visual Characterization

SEM images of cut and polished surfaces confirmed that the specimens contained 40% by volume glass beads. No regions of excess particle agglomeration were seen in any of the specimens.

The SEM photographs in Figure 1 are the fracture surfaces of composites containing untreated and treated glass beads. Without the coupling agent [Fig. 1(a)], fracture of the specimen apparently produced clean separation of the glass beads from the matrix, and cracks or voids between remaining glass beads and the matrix can be clearly seen. The overall appearance of the surface is characteristic of brittle fracture. With the silane coupling agent [Fig. 1(b)], fracture leaves a significant amount of matrix adhering to glass bead surfaces. The surface appearance implies greater ductility. These observations are consistent with the assumption that the silane coupling agent is covalently bound to both the matrix and the glass beads.

Water Uptake

Upon exposure to distilled water, all specimens manifested weight increases due to water uptake. Figure 2 shows the average percent weight increase, relative to the dry matrix weight, of the plain matrix, the untreated composite, and the silane-treated composite. For the first 300 h, the weight increase was proportional to the square root of time, suggesting that a Fickian diffusion model describes water uptake during the early stages of soaking. The linear portions of the uptake curves for the untreated composite and the plain matrix have similar slopes;

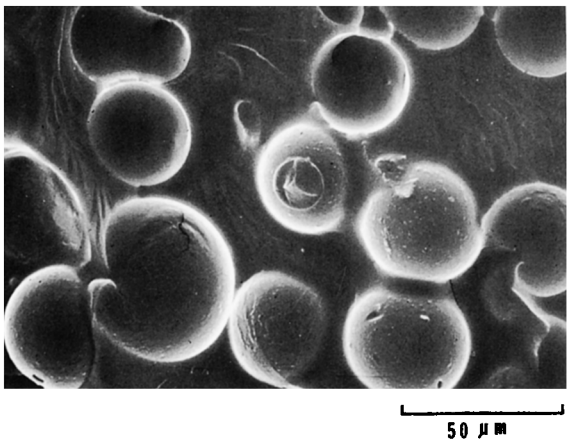

Figure 1 Scanning electron micrographs of the fracture surfaces of (a) an untreated composite specimen (×500) and (b) a silane-treated composite specimen (×500).

thus, water transport through the matrix controls the water uptake process. The lower water uptake rate by the treated composite may be due to alterations of the matrix structure by the coupling agent.

After 1500 h, the specimens were saturated with water. The saturated water content (weight percent based on initial matrix weight) for plain matrix, untreated composite, and silane-treated composite were 3.32 ± 0.14, 5.68 ± 0.14, and 2.58 ± 0.20, respectively.

The larger water content of the untreated composite can be attributed to the poor adhesion between the glass beads and the matrix. Without chemical bonding between the glass and the matrix, the exposed hydrophilic sites on the glass surface attracted water. Dissolution of ionic groups would increased the osmotic pressure; subsequent water uptake further dilated the interstitial voids in the interphase. In the silane-treated composite, the chemical bonds between the silane and the glass reduced the number of the hydrophilic sites and, thus, the amount of water uptake. The strength of the matrix-glass bond resisted moisture-induced dilation. The SEM micrographs (Fig. 1) support this rationalization: the untreated composite had distinct cracks at the glass–matrix interface, but the silane-treated composite did not.

The plain matrix absorbed more water than the silane-treated composite. The silane may have introduced additional crosslinking in the matrix near the glass surface. The local densification in the interphase would reduce the free volume available for water, perhaps explaining the observed difference in the water uptake. Alternately, the chemical composition of the interphase could simply be less hydrophilic than the plain matrix.

DMA Temperature Sweep Results

The viscoelastic mechanical properties of polymer matrix composites arise from the polymeric nature of the matrix. Because polymer relaxation processes are highly temperature dependent, temperature ramp tests are especially well suited for characterizing energy dissipation associated with polymer relaxation processes. The loss tangent [eq. (4)] is particularly informative for this purpose.

General Features and Reproducibility

Figure 3 shows the temperature dependence of the storage modulus and loss tangent for four duplicate specimens of the water-soaked untreated composite. Decreases in the storage modulus and associated peaks in the loss tangent identify three major relaxation processes. The largest peak in the loss tangent, denoted as the α-relaxation, is associated with the glass transition of the polymer matrix at about 120°C. The broad peak centered at about −40°C,

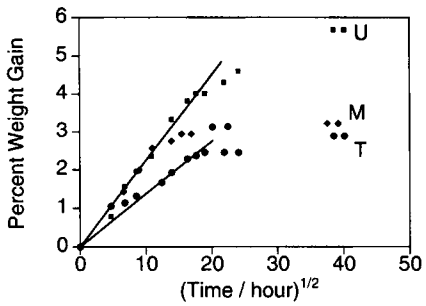

Figure 2 Percent weight increase due to water uptake vs. square root of time for plain matrix (*M*), untreated composite (*U*), and treated composite (*T*).

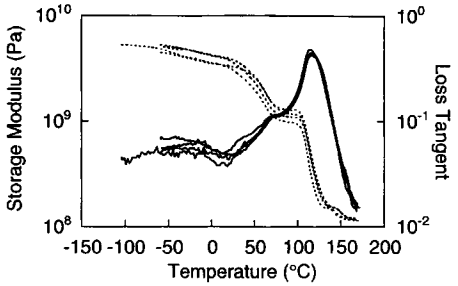

Figure 3 Duplicate temperature sweep measurements of the storage modulus (dashed curves) and loss tangent (solid curves) of the water-soaked, untreated composite.

labeled the β-relaxation, has been attributed to rapid, small-scale motions of the polymer molecules.[26] The drop in the storage modulus between 25 and 75°C indicates a third relaxation that has been called the ω-relaxation.[13,27] The magnitude of the associated loss tangent peak has previously been associated with water uptake.[27] We denote the temperatures of the loss tangent peaks for these relaxations with the appropriate subscript (α, β, or ω).

The duplicate temperature sweeps shown in Figure 3 reveal some variability in the magnitude of the storage modulus, although the shapes of the curve are quite similar. Slight variations in the thickness of the specimens could account for the differences. The loss tangent, however, is insensitive to specimen thickness because it equals the ratio of moduli [eq. (4)]; consequently, the loss tangent curves in Figure 3 display less variability than the storage modulus curves.

We observed a similar degree of reproducibility for all classes of specimens. To compare the properties of different classes of specimens, we select values of the storage modulus and loss tangent at particular points in the temperature sweep. Specifically, we compare values of the storage modulus at −30, 75, and 160°C. For the loss tangent, the temperature and peak value of the α-relaxation will be compared, as well as the loss tangent at 75°C. All comparisons are stated with a confidence level of 99% or greater unless otherwise noted.

Atmosphere-Conditioned Specimens

Table I reports the average viscoelastic properties of atmosphere-conditioned plain matrix, untreated composite, and treated composite specimens. The composites' storage moduli at all temperatures are greater than those of the plain matrix as a consequence of the reinforcing effect of the glass beads.

The storage modulus of the treated composite was certainly greater than that of the untreated composite at 160°C. At lower temperatures, the differences between the storage moduli of the composites were small: at 75°C, there was no difference, and at −30°C, the treated composite's modulus was greater, although the statistical certainty was only about 80%. In the silane-treated composite, crosslinking between the matrix and the glass beads presumably enabled more efficient transfer of the applied load between the matrix and the glass, thus increasing the storage moduli. However, the low statistical significance of the comparisons at temperatures below T_α mitigate against the use of storage moduli for assessing the effect of interfacial structure on composite properties.

The addition of glass beads to the polymer matrix caused a small but statistically significant decrease in T_α. Lower values of T_α are presumably associated with greater molecular flexibility. However, it is difficult to rationalize this with a greater degree of crosslinking in the interphase. Nevertheless, the decrease in T_α was greater for the untreated composite than for the treated composite, suggesting that differences in the structure in the glass–matrix interphases were responsible.

The loss tangent sat 75°C and at T_α were much less in the composites than in the plain matrix. Energy dissipation per unit volume in the composites was less because the rigid glass beads did not dissipate mechanical energy and occupied 40% of the composites' volume.

Table I Dynamic Mechanical Properties of Atmosphere-Conditioned Specimens[a]

Class	Storage Modulus (10^8 Pa)			Loss Tan.		Loss Tan.
	−30°C	75°C	160°C	75°C ($\times 10^{-2}$)	T_α (°C)	at T_α
Plain matrix	30.9 ± 1.4	16.7 ± 0.5	0.45 ± 0.02	4.20 ± 0.47	132.9 ± 0.3	0.753 ± 0.017
Untreated comp.	45.9 ± 4.2	28.9 ± 2.0	1.67 ± 0.18	3.34 ± 0.47	129.2 ± 0.5	0.574 ± 0.008
Treated comp.	48.6 ± 8.8	28.8 ± 4.9	1.97 ± 0.24	2.96 ± 0.40	130.7 ± 1.3	0.547 ± 0.011

[a] Averages of measurements from 10 duplicate specimens.

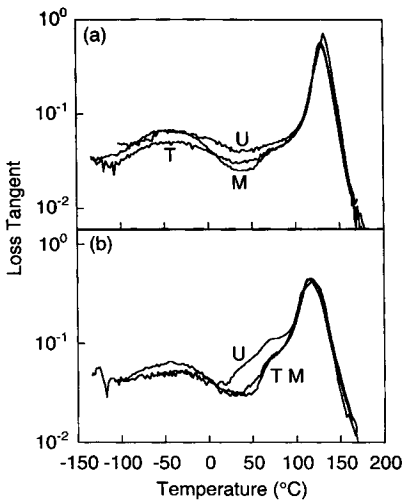

Figure 4 Temperature dependence of the loss tangent for plain matrix (*M*), untreated composite (*U*), and treated composite (*T*), for (a) atmosphere-conditioned specimens and (b) water-soaked specimens.

More importantly, the treated composite had significantly lower loss tangents at 75°C and at T_α than the untreated composite (>97% confidence at 75°C). The greater degree of crosslinking in the treated composite, either between the glass and the matrix or solely within the matrix, lowered the volumetric rate of energy dissipation. Values of the loss tangent, thus, provide a good measure of the contribution of interfacial structure to the mechanical properties of our composites.

Figure 4(a) compares the loss tangent spectra for specimens of dry plain matrix, untreated composite, and treated composite. The significant features associated with the α-relaxation were discussed earlier. The loss tangents of these specimens appear to differ considerably below 100°C. Comparison of average loss tangent values indicate lower values for composites compared to plain matrix (Table I). However, Figure 4(a) does not show any significant difference between the loss tangents of treated and untreated composites below 100°C for these particular specimens.

All of the loss tangent spectra in Figure 4(a) display an ω-relaxation peak at the left shoulder of the α-relaxation peak. We suspect that these nominally dry specimens actually contained water absorbed from the ambient air, and that this water was responsible for the ω-relaxation peak. To test this hypothesis, we subjected a fresh "dry" plain matrix specimen to two sequential temperature-ramp tests. Comparison of the two spectra revealed that the ω-relaxation peak vanished in the second test, implying that the temperature ramp of the first test removed the water in the "dry" specimen. Also, once-tested dry specimens were retested after several months of exposure to ambient air; the specimens again displayed the ω-relaxation peak. Last, a "dry" specimen was dried in a vacuum oven for 20 min and then tested: the loss tangent spectrum did not display an ω-relaxation peak. These tests confirm our hypothesis that absorbed water from the ambient air causes the small ω-relaxation peak in our nominally dry specimens.

Water-Soaked Specimens

Table II shows the average values of the viscoelastic properties of water-soaked plain matrix, untreated composite, and treated composite specimens. As expected, all of the composite storage moduli were greater than those of the plain matrix (except for untreated composite at 75°C). Furthermore, the storage moduli of the treated composite were all greater than those of the untreated composite. The silane coupling agent created additional interfacial crosslinking in the treated composite, leading to efficient load transfer between the matrix and the reinforcing glass and, thus, higher moduli.

At temperatures below 0°C, the loss tangents of the wet composites were less than that of the wet plain matrix due to the lack of viscous dissipation in the elastic glass beads. However, we could not

Table II Dynamic Mechanical Properties of Water-Soaked Specimens[a]

Class	Storage Modulus (10^8 Pa)			Loss Tan.		Loss Tan.
	−30°C	75°C	160°C	75°C ($\times 10^{-2}$)	T_α (°C)	at T_α
Plain matrix	28.9 ± 2.9	13.9 ± 0.9	0.46 ± 0.03	8.03 ± 0.26	119.8 ± 4.0	0.440 ± 0.020
Untreated comp.	44.0 ± 3.8	12.3 ± 1.4	1.20 ± 0.02	11.36 ± 0.21	115.8 ± 1.2	0.446 ± 0.020
Treated comp.	56.6 ± 2.7	29.6 ± 0.9	1.67 ± 0.03	7.58 ± 0.51	113.9 ± 0.9	0.421 ± 0.017

[a] Averages of measurements from 10 duplicate specimens.

discern any significant difference between the loss tangents of the treated and untreated composites at low temperatures. Significant differences in T_α and the maximum value of the loss tangent in the α-relaxation peak were observed (Table II): the silane-treated composite had the lowest values of T_α and loss tangent at T_α, both consistent with greater crosslinking at the glass–matrix interface. However, we could not control the rate at which specimens lost water during DMA testing at temperatures above 100°C; the corresponding loss tangent data should, therefore, be viewed with some suspicion.

The most significant features of the loss tangent curves for the wet specimens were the large ω-relaxation peaks between 20 and 80°C. For example, Figure 4(b) compares the loss tangent spectra for specimens of wet plain matrix, untreated composite, and treated composite. The plain matrix and treated composite specimens displayed similar, distinct ω-relaxation peaks centered at about 70°C. The ω-relaxation peak seen in the untreated composite was much larger, however. Figure 3 demonstrates that the untreated composite's ω-relaxation peak was quite reproducible.

Comparison of loss tangent values at 75°C (Table II) shows that the wet-treated composite had a loss tangent significantly less than that of the wet-plain matrix, but the loss tangent of the untreated composite was much higher. In view of the water uptake data shown in Figure 2, we conclude that the magnitude of the ω-relaxation peak in the loss tangent correlates with the amount of water absorbed by the specimen.

The mechanism by which water creates and amplifies the ω-relaxation has not been established. The appearance of this additional peak in the presence of water suggests a distinctive, water-mediated relaxation process. One could view this relaxation as the α-transition of a polymeric phase containing a higher water concentration than that of the matrix, on average. Absorbed water may concentrate near hydrophilic sites in the polymer, in microvoids, or in cracks or debonds at the glass–matrix interface. The water-saturated microdomains would have a lower glass transition temperature, and plasticization by the water would increase viscous dissipation and the loss tangent. These features are consistent with those of the ω-relaxation peak seen in Figures 3 and 4(b).

On the other hand, significant water may have been driven out of the specimens during the course of the temperature sweep tests. The enhanced ω-relaxation peak may reflect the effects of water transport on the α-transition of an otherwise uniform matrix structure. Multiple relaxation peaks have been shown to be artifacts of temperature sweep tests conducted at high temperature ramp rates.[8] Therefore, caution must be exercised when proposing mechanistic interpretations of the effect of water on loss tangent data. Regardless of the mechanism, though, the correlation between surface treatment of the glass beads, water uptake, and magnitude of the ω-relaxation peak is unambiguous.

Comparison of Dry and Wet Specimens

Figure 5 compares the storage modulus and loss tangent spectra of dry and wet plain matrix, dry and wet untreated composite, and dry and wet silane-treated composite. In general, water plasticized the matrix, shifting the α-relaxation peak of all dry specimens lower by about 15°C. The values of the loss tangent at T_α were smaller for all wet specimens than for the dry ones. Bearing in mind the uncertainty of the water content at temperatures greater than 100°C, the lower values of the loss tangent at T_ω could be due to the plasticizing effect of water.

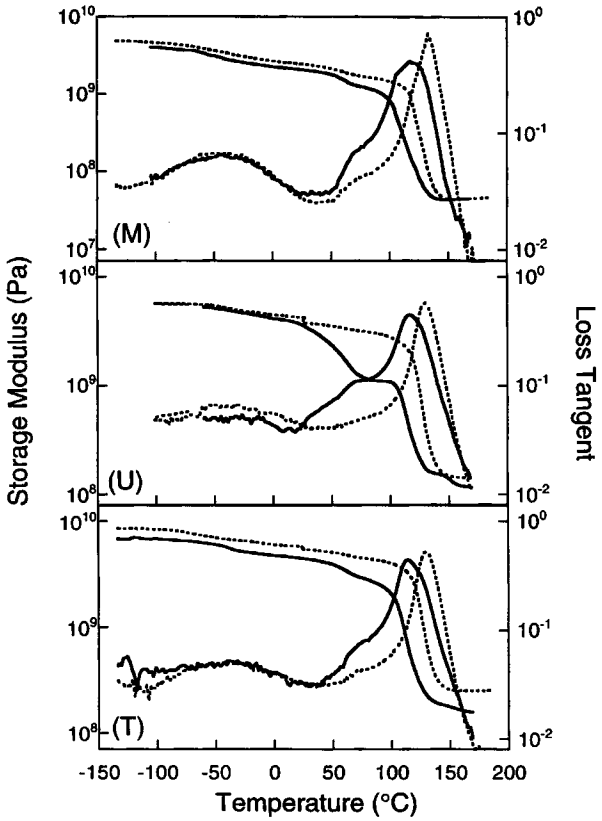

Figure 5 Effect of water uptake on the storage modulus and loss tangent for plain matrix (*M*), untreated composite (*U*), and treated composite (*T*); dashed curves are for dry specimens, solid curves are for wet specimens.

If water disrupted the intermolecular attraction between polymer molecules, then the matrix would have behaved more like an elastic network constrained only by chemical crosslinks. Hence, the loss tangent values should be lower for the wet specimens, and the α-relaxation peaks should occur at lower temperatures.

However, water did not significantly alter the β-relaxation peak. The β-relaxation involves rapid, small-scale motions due to bond bending and rotation, rather than gross translational motions associated with the α-relaxation. We believe that the insensitivity of the β-relaxation peak to water content indicates that water did not significantly alter local molecular motion in the polymer matrix.

Water had a profound effect upon the shape and magnitude of the ω-relaxation peak in the loss tangent (Fig. 5). In all cases, water increased the magnitude of the ω-relaxation peak for the wet specimens compared to the dry ones. The increase was comparable for the plain matrix and the treated composite, but it was much greater for the untreated composite. This trend correlates with the measured water content of the specimens (Fig. 2). As discussed in the previous section, these observations support the hypothesis that poor interfacial adhesion in the untreated composite led to greater water uptake, and that the water content controlled the magnitude of the ω-relaxation peak in the loss tangent.

Specimen-to-specimen variability mitigates against direct comparison of the magnitudes of the storage moduli shown in Figure 5. However, we may compare the average values reported in Tables I and II. At $-30°C$, the storage moduli of wet plain matrix and untreated composite were comparable to the values for dry specimens. The storage modulus at $-30°C$ of the wet-treated composite was significantly higher than that of the dry-treated composite. We cannot explain the apparent reinforcing effect of water in the silane-treated composites.

For specimens at 75°C, water reduced the storage modulus of plain matrix by 17% (compared to dry) and of untreated composite by 57%. In fact, the high water content of the untreated composite gave it a lower storage modulus than plain matrix at this temperature. However, water may have slightly increased the storage modulus of treated composite (70% statistical certainty).

The storage moduli of the wet and dry plain matrix at 160°C were identical. At this point in the temperature ramp tests, unknown amounts of water may have been driven out of the samples. The storage moduli of the wet composites were smaller than those of the dry composites at 160°C, consistent with plasticization of the rubbery matrix by water. The glass beads in the composites my have hindered water transport out of the specimens, leaving sufficient residual moisture to account for the lower moduli. Alternately, if most of the water had left the specimens, the decreased moduli could reflect interfacial debonding or other damage in the composites. Unfortunately, we did not address this question by testing specimens that had been soaked and then redried to zero water content.

DMA Frequency Sweep Results

Master Curves

For all specimens, time–temperature superposition produced storage modulus master curves that varied smoothly and continuously with frequency. All of the master curves for the composite specimens gave higher storage moduli than the master curves for plain matrix, as expected.

Figure 6(a) shows storage modulus master curves for representative specimens of dry-untreated and -treated composites. Identical specimens should have identical master curves. Instead, the treated composite had a greater storage modulus for frequencies less than 10^{20} s^{-1}. This may reflect the greater degree of interfacial crosslinking in the treated composite.

The effect of water on typical treated and untreated composites is illustrated in Figure 6(b). Again, differences due to the silane coupling agent are apparent. At high frequencies, the treated composite had a greater storage modulus. Water altered

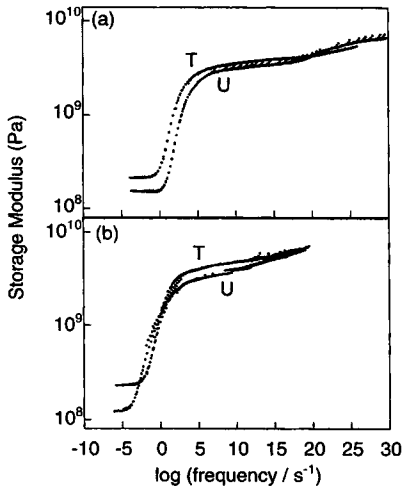

Figure 6 Storage modulus master curves for (a) dry- and (b) wet-treated and -untreated composite (denoted *T* and *U*, respectively).

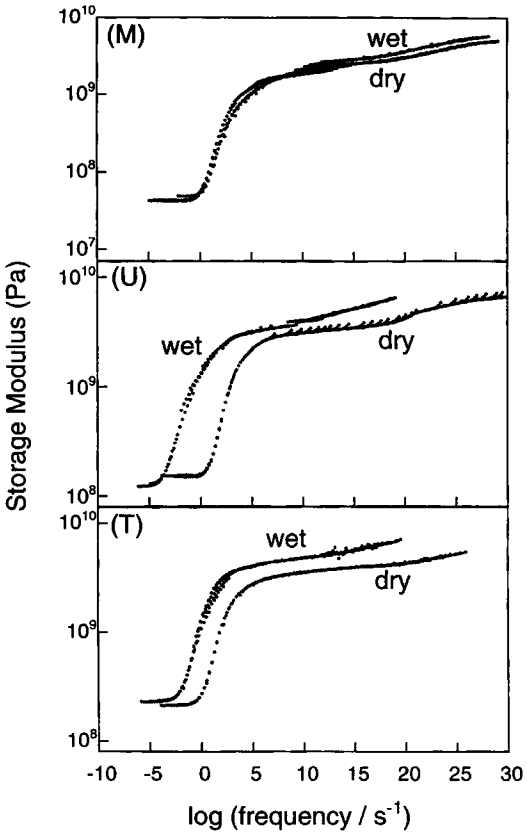

Figure 7 Effect of water uptake on storage modulus master curves for plain matrix (*M*), untreated composite (*U*), and treated composite (*T*).

the shape of the untreated composite's master curve in the region of the glass transition and reduced its rubbery modulus. However, we must be cautious when comparing the low frequency, high temperature portions of master curves for wet specimens: we found that frequency sweeps at higher temperatures were particularly prone to water loss. Still, for both dry and wet composites, we see that the master curves manifest differences in interfacial structure.

Direct comparisons of dry and wet specimens are shown in Figure 7. For the plain matrix [Fig. 7(a)], the master curves nearly superimpose, suggesting that time–temperature–*moisture* superposition might be applicable. We call these materials "thermo-rheologically similar." The corresponding shift factor–temperature curves [Fig. 8(a)] show that at low temperatures, the values of $\ln(a_T)$ differ by a constant, consistent with unchanging water content in the wet plain matrix. At temperatures greater than ambient, the shift factor curves merge, suggesting that the wet plain matrix lost water.

The storage modulus master curves for the dry- and wet-treated composites [Fig. 7(b)] did not superimpose: these materials were not thermo-rheologically similar. Unlike the wet plain matrix, the water distribution in the composite may not have been homogeneous. The values of the shift factor [Fig. 8(b)] differ under most conditions but coincide at the highest temperatures, again suggesting water loss by the wet specimen. The untreated composites were not thermo-rheologically similar either: we see even greater differences between the storage modulus master curves for dry and wet untreated composite [Fig. 7(c), presumably due to the higher water content of the wet specimen relative to the dry one. The corresponding shift factors [Fig. 8(c) clearly differ in magnitude by a constant at low temperatures, but begin to merge above 70°C.

Apparent Activation Energies

The shift factor–temperature relationship can be used to determine apparent activation energies for polymer relaxation processes. Although mechanistic interpretations of apparent activation energies are

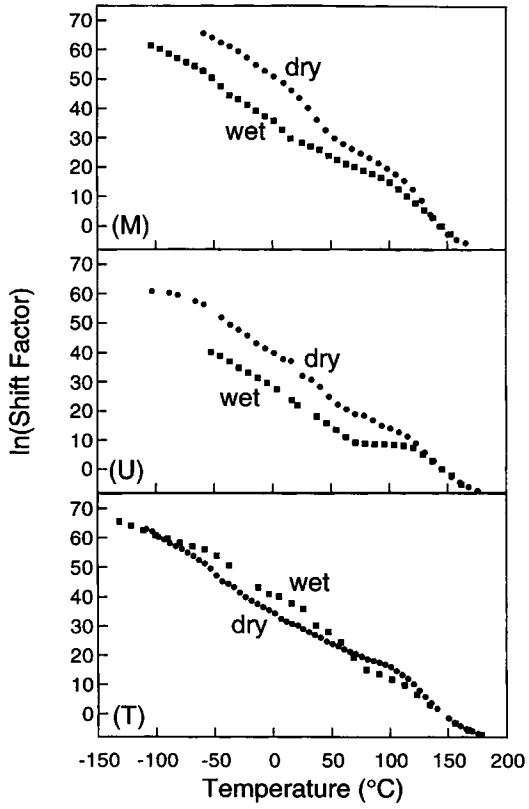

Figure 8 Effect of water uptake on shift factor–temperature curves for plain matrix (*M*), untreated composite (*U*), and treated composite (*T*).

possible, we use them here primarily for comparative purposes. Shift factor–temperature data, plotted according to the Arrhenius equation,

$$\ln(a_T) = \frac{E_\beta}{R}\left(\frac{1}{T} - \frac{1}{T_R}\right) \quad (5)$$

has been used to identify the apparent activation energy associated with the β-relaxation process, E_β.[21] Least squares fits of shift factor–temperature data between −60 and 0°C, plotted according to eq. (5), gave straight lines with regression coefficients close to unity for all classes of specimens.

Average values of E_β are given in Table III. For both dry and wet specimens, E_β was lowest for the treated composite (although the statistical certainty was not very high for some of the comparisons among the dry specimens). Greater interfacial crosslinking in the treated composite could account for this observation. Water seemed to have little effect upon E_β for the plain matrix or the treated composite, but E_β was much greater for the wet untreated composite compared to the dry. Values of E_β for the wet specimens correlate with the saturated water content. We speculate that relatively large amounts of "frozen" water in the untreated composite hinder local molecular motions associated with the β-relaxation.

At temperatures around the α-relaxation, the empirical WLF equation[28]

$$\log(a_T) = -C_1\left(\frac{T - T_R}{C_2 + T - T_R}\right) \quad (6)$$

has successfully been used to describe the temperature dependence of shift factors for molten or rubbery polymers. The constants C_1 and C_2 were extracted from plots of $1/\log(a_T)$ vs. $1/\log(T - T_R)$. Such plots yielded straight lines with regression coefficients close to unity only for dry specimens. An apparent activation energy for the α-relaxation, E_α, was computed from:[11,21]

$$E_\alpha = R\frac{d[\ln(a_T)]}{d(1/T)}\bigg|_{T=T_R} = 2.303\mathrm{R}\frac{C_1 T_R^2}{C_2}. \quad (7)$$

For wet specimens, water loss during the experiments did not permit identification of E_α in this way.

Table III contains values of E_α for dry specimens. The value of E_α was greatest for the plain matrix and least for the untreated composite, suggesting that large-scale motions of polymer molecules occurred more easily in the latter than in the former. Two explanations seem plausible. First, residual stresses due to differential thermal expansion between the glass and the matrix were present in the composites but not in plain matrix. Second, the glass beads eliminated some of the crosslinks that the polymer would have had in the plain matrix. Both residual stresses and reduced crosslink density may have enabled large-scale molecular motion in the composites at lower temperatures and applied strains. The greater value of E_α for the dry-treated composite than that of the untreated composite was presumably due to lower residual stresses and greater interfacial crosslinking in the former. Regardless of the mechanism, we conclude that apparent activation energies are sensitive to water content and interfacial characteristics in these materials.

CONCLUSIONS

The objective of this study was to correlate the results of dynamic mechanical testing with water uptake and interfacial structure of glass bead–epoxy matrix composites. In addition to specimens of plain cured matrix, we fabricated composites containing either clean glass beads ("untreated"), or glass beads treated with a silane coupling agent ("treated"). Our goal was to create composites with ostensibly poor and good interfacial adhesion.

SEM visualization of fracture surfaces revealed apparent interfacial debonding in the untreated composite that was not observed in the treated com-

Table III Apparent Activation Energies and Saturated Water Contents[a]

Class	E_β (kcal/mol) (dry)	E_β (kcal/mol) (wet)	E_α (kcal/mol) (dry)	Water Content (%)
Plain matrix	33.8 ± 4.6	33.8 ± 1.9	143 ± 14	3.22 ± 0.14
Untreated composite	31.7 ± 4.0	36.2 ± 4.7	112 ± 12	5.68 ± 0.14
Treated composite	29.8 ± 2.6	30.7 ± 3.3	126 ± 10	2.58 ± 0.20

[a] Averages of measurements from 10 duplicate specimens.

posite. Water uptake measurements indicated that the untreated composite absorbed much more water than either the plain matrix or the treated composite. Poor glass–matrix adhesion in the untreated composites can account for these observations. On the other hand, visual characterization of the apparent ductile fracture of treated composites, and their low water uptake compared to plain matrix, are consistent with the view that the silane coupling agent creates more crosslinks in the interfacial region, either between the glass and the epoxy, or within the epoxy.

We conducted dynamic mechanical tests of atmosphere-conditioned ("dry") and water-soaked specimens of plain matrix, untreated composites, and treated composites. From temperature sweep tests, we measured spectra of loss and storage modulus as well as their ratio, the loss tangent. From frequency sweep tests, we constructed master curves through time–temperature superposition, thereby identifying shift factor–temperature relationships. Through the use of the Arrhenius and WLF equations, we extracted the apparent activation energies of polymer relaxations in our specimens.

For the dry specimens, glassy storage moduli and T_α displayed some sensitivity to the presence of silane coupling agent. However, the statistical certainty associated with storage modulus comparisons was relatively poor due to specimen-to-specimen variations. Because the properties of the matrix control T_α, we do not consider it to be a good parameter for characterizing interfacial structure. Instead, the value of the loss tangent at T_α proved to be quite sensitive to the presence of the silane.

The plasticizing effect of water shifted T_α lower by about 15°C for all specimens. The values of T_α and the loss tangent at T_α were sensitive to the quality of interfacial adhesion in wet composites. Most importantly, temperature sweep tests identified an additional relaxation process denoted as the ω-relaxation. The magnitude of the ω-relaxation correlated with the amount of water absorbed by the specimen. Because water uptake depends on the quality of interfacial adhesion, the magnitude of the ω-relaxation may be a useful measure of interfacial adhesion.

The features of master curves from frequency sweep tests also manifested the effect of water uptake and interfacial structure. However, it is difficult to rationalize the differences between master curves in terms of molecular mechanisms. Furthermore, shift factor data suggest that temperature sweep experiments were more prone to water loss over the course of the experiment. For dry specimens, apparent activation energies associated with the α-relaxation reflected differences between plain matrix and composites, and between composites with ostensibly poor and good interfacial adhesion. For wet specimens, the apparent activation energy associated with the β-relaxation correlated with water uptake and, indirectly, interfacial adhesion. For composites with finer gradations in interfacial adhesion, however, the activation energies may lack the desired sensitivity.

In summary, we recommend the use of the loss tangent at T_α as the best parameter for characterizing variations in interfacial structure in dry composites. For wet composites, the magnitude of the loss tangent in the ω-relaxation peak was most sensitive to water content and interfacial adhesion. Experiments are currently in progress to calibrate these measures with varying amounts of interfacial damage in fiber-reinforced epoxy matrix composites.

We gratefully acknowledge the financial support of the Offshore Technology Research Center and the National Science Foundation through the Engineering Research Center grant #CDR-8721512.

REFERENCES

1. G. S. Springer, *Environmental Effects on Composite Materials,* Technomic, Westport, CT, 1981; J. C. Halpin, in *The Role of the Polymeric Matrix in the Processing and Structural Properties of Composite Materials*, J. C. Seferis and L. Nicolais, Eds., Plenum, New York, 1983.
2. N. M. Cameron, *Glass Technol.*, **9,** 121 (1968).
3. W. D. Bascom, in *Interfaces in Polymer Matrix Composites,* E. P. Plueddemann, Ed., *Composite Materials,* Vol. 6, Academic, New York, 1974.
4. L. T. Drzal, *Adv. Polym. Sci.*, **75,** 1 (1986).
5. E. G. Wolff, *SAMPE J.*, **29,** 11 (1993).
6. M. R. Piggott, in *Advances in Composites: Chemical and Physicochemical Effects,* T. L. Vigo and B. Kinzig, Eds., VCH, New York, 1991.
7. P. S. Chua, S. R. Dai, and M. R. Piggott, *J. Mater. Sci.*, **27,** 919 (1992).
8. J. L. Thomason, *Polym. Comp.*, **11,** 105 (1990).
9. T. B. Lewis and L. E. Nielsen, *J. Appl. Polym. Sci.*, **14,** 1449 (1970).
10. P. S. Chua, *Polym. Comp.*, **8,** 308 (1987).
11. N. Amdouni, H. Sautereau, and J. F. Gerard, *J. Appl. Polym. Sci.*, **45,** 1799 (1992).
12. J. Hilborn, J. E. Bidaux, and J. A. E. Manson, *ACS Polym. Prepr.*, **34,** 639 (1993).
13. J. F. Gerard, *Polym. Eng. Sci.*, **28,** 568 (1988).
14. B. Harris, O. G. Braddell, D. P. Almond, C. Lefebvre, and J. Verbist, *J. Mater. Sci.*, **28,** 3353 (1993).

15. J. F. Gerard, S. J. Andrews, and C. W. Macosko, *Polym. Comp.*, **11,** 90 (1990).
16. J. M. Kennedy, D. D. Edie, A. Banerjee, and R. J. Cano, *J. Comp. Mater.*, **26,** 869 (1992).
17. S. Dong and R. Gauvin, *Polym. Comp.*, **14,** 414 (1993).
18. J. Y. Wang, MS Thesis, Texas A&M University, 1994.
19. J. G. Williams, *J. Mater. Sci.*, **17,** 1427 (1982).
20. G. C. Papanicolaou and A. Pappa, *J. Mater. Sci.*, **27,** 3889 (1992).
21. J. D. Ferry, *Viscoelastic Properties of Polymers,* Wiley, New York, 1980.
22. C. L. Schutte, preprint, *Mater. Sci. Eng. Rep.*, 13, 7, Nov 15 (1994).
23. T. Marzi, U. Schroder, M. Hess, and R. Kosfeld, *Mater. Res. Soc. Symp. Proc.*, **170,** 123 (1990).
24. U. Schroder, T. Marzi, M. Hess, and R. Kosfeld, *Mater. Res. Soc. Symp. Proc.*, **170,** 129 (1990).
25. S. L. Simon and J. K. Gillham, *J. Appl. Polym. Sci.*, **46,** 1245 (1992).
26. J. G. Williams, *J. Appl. Polym. Sci.*, **23,** 3433 (1979).
27. J. D. Keenan, J. C. Seferis, and J. T. Quinlivan, *J. Appl. Polym. Sci.*, **24,** 2375 (1979).
28. M. L. Williams, R. F. Landel, and J. D. Ferry, *J. Am. Chem. Soc.*, **77,** 3701 (1955).

Received March 31, 1995
Accepted July 30, 1995